INFLUENCE OF ANNEALING TEMPERATURE AND ATMOSPHERE ON THE MORPHOLOGY AND LUMINESCENT PROPERTIES OF NANOSTRUCTURED MATERIALS

Viktor Zavodyannyi[1]*, Mykola Voloshyn[1], Valentina Zubenko[1], Roman Kovalenko[1], Serhii Rahulin[1]

[1]Department of Hydraulic Construction, Water and Electrical Engineering, Kherson State Agrarian and Economic University, Kropyvnytskyi, Ukraine

(ORIGINAL SCIENTIFIC PAPER)
UDC: 66,017/018
DOI: 10.5937/savteh2601057Z

The aim of the study was to determine how the temperature and gaseous environment of annealing affect the morphological and luminescent properties of nanostructured zinc oxide (Zn) -based materials. The study was carried out in Ukraine at the National Technical University of Ukraine "Igor Sikorsky Kyiv Polytechnic Institute". The methodology included chemical deposition from aqueous solutions followed by thermal annealing at 300, 500, and 700 °C in air, nitrogen, and argon. The morphology was analysed by scanning electron microscopy (SEM), the crystal structure by X-ray diffraction (XRD), and the luminescence spectra by photoluminescence (PL) spectroscopy. The results showed an increase in particle size with increasing temperature, regardless of the atmosphere, with a minimum (~45 nm) at 300 °C in argon and a maximum (~112 nm) at 700 °C in air. With increasing temperature, the coverage density decreased, especially under inert conditions, due to nanoparticle aggregation. Correlation analysis showed a strong negative relationship between particle size and emission intensity (r=-0.89) and a positive correlation between coverage density and PL brightness (r=0.76). Thus, it was established that high-temperature annealing in an oxygen atmosphere most effectively improves the luminescent characteristics of ZnO for optoelectronic and sensor applications. The results are of practical significance for the development of high-efficiency optoelectronic and sensing devices.

Keywords: layer density, spectral purity, crystallite size, emission intensity, lattice defects, Zinc oxide

Introduction

ZnO, as a nanostructured material, has attracted increased attention from the scientific community over the last two decades (2000-2020) owing to its unique combination of electronic, optical, and morphological properties, which are key to a wide range of applications, in particular in optoelectronics, photocatalysis, biosensing, and luminescent devices. Of considerable scientific interest is the possibility of regulating these properties by controlling the technological parameters of synthesis and heat treatment. One of the key stages in forming the target characteristics of ZnO is thermal annealing, which affects the structure, structural defects, crystallinity, and, as a consequence, the luminescent efficiency of the material. Despite the large number of studies in this field, several unresolved issues remain related to the relationship between the annealing conditions – particularly temperature and gaseous atmosphere – and the resulting morphological and optical properties of ZnO nanostructures.

A crucial scientific task is to clarify the regularities that describe the influence of different annealing atmospheres on nanoparticle aggregation and the stability of the luminescent response. This problem is particularly important in cases where it is necessary to ensure high emission brightness while maintaining a nanoscale structure. Vasin *et al*. [1] investigated the influence of inert and oxidising gases on the luminescence of ZnO, showing that in argon, there is an increase in defect luminescence due to limited repassivation of surface states. However, the results obtained showed variability depending on temperature, which complicates the formulation of unambiguous generalisations. Thus, there remained a need for a comprehensive analysis of morphology and spectral characteristics under strictly controlled conditions.

Another critical problem is the dependence of crystallite and particle size on annealing temperature and the influence of this parameter on the quality of the crystal lattice [2-5]. Michailovska *et al.* [6] demonstrated that increasing temperature promotes crystallite growth and a reduction in defects in the structure, but these observations were made only under air-atmosphere conditions, which limits the robustness of the conclusions. In ad-

***Author address**: Viktor Zavodyannyi, Department of Hydraulic Construction, Water and Electrical Engineering, Kherson State Agrarian and Economic University, 25031, 5/2 Universytetskyi Ave., Kropyvnytskyi, Ukraine;
e-mail address: vzavodyannyi@gmail.com
The manuscript received: 23.12. 2025
Paper accepted: 15.05. 2025

dition, the influence of changes in coating morphology on functional properties such as PL was not analysed, which limits a comprehensive understanding of the interdisciplinary relationships in material behaviour.

The literature often contains the hypothesis of an inverse correlation between nanoparticle size and PL intensity [7]. However, confirmation of this statement requires precise quantitative analysis. Kryshtab et al. [8] carried out a correlation study between the morphological and optical parameters of ZnO obtained by different synthesis methods, but the absence of systematic variation of thermal-treatment conditions limited the scope of the information obtained. Moreover, changes in coverage density were not taken into account, which, as later emerged, significantly influence collective optical effects.

Another problem concerns the role of the annealing atmosphere in forming the defect structure of ZnO. For example, in reducing or inert conditions, oxygen vacancies (V_O) or other defects may form, which substantially alter the material's spectral properties. Talla et al. [9] examined the mechanisms of formation of such defects and showed that the intensity depends not only on temperature but also on the cooling rate after annealing. However, the approach was based on modelling, without experimental confirmation over a wide temperature range, which leaves room for practical verification.

A pressing issue remains the optimisation of the structural order of the material without a concomitant increase in particle size, which is particularly important for the development of efficient nanomaterials. Buryi et al. [10] investigated the influence of stepwise temperature increase on the crystallinity of ZnO, finding that gradual annealing contributes to a reduction in the size of defective regions. However, the absence of analysis of the morphological consequences of such regimes and the impact on the coating did not allow a complete picture to be formed of the relationships between the micro- and nanoscale levels of structure.

Another line of research is the evaluation of the effectiveness of different atmospheres in ensuring high emission brightness with minimal peak broadening. Desouky and Abou-Helal [11] compared the PL properties of ZnO after annealing in nitrogen and oxygen, pointing to the advantages of oxidising conditions. However, the study lacked information on the morphology of the samples, and it did not consider how particle size correlates with the width and shape of spectral peaks.

The problem of consistency between the morphological, structural, and optical characteristics of ZnO still remains relevant. Sharma and Sahare [12] in their studies focused on spectral analysis, finding a relationship between the width of the UV peak and the level of order of the crystal lattice. However, the results were obtained on the samples synthesised by the hydrothermal growth method, which significantly limits the extrapolation of the conclusions to other methods of obtaining nanostructures.

Finally, a key problem is the insufficient number of studies in which the morphological, crystalline, and luminescent properties of ZnO are analysed simultaneously under the influence of different annealing temperatures and atmospheres. Roselló-Márquez et al. [13] attempted a comprehensive analysis of the morphological, crystalline, and luminescent properties of ZnO, but the analysis was fragmentary: correlation dependencies between the parameters were not taken into account, and the optimal conditions for achieving high PL efficiency while maintaining a nanoscale structure remained undefined.

Considering the above research limitations, a systematic study becomes relevant that will make it possible to establish clear relationships between annealing temperature, gaseous atmosphere, and the resulting morphological and luminescent characteristics of nanostructured ZnO. For this reason, the aim of the study was to determine the influence of the temperature and composition of the thermal-annealing atmosphere on the morphology and luminescent properties of nanostructured oxide materials based on ZnO. The objectives of the study included the analysis of coating morphology, the determination of crystal structure, the investigation of PL spectra, and the establishment of statistical correlations between the obtained parameters.

Materials and methods

The research was conducted from March to November 2023 at the Department of Solid State Physics, National Technical University of Ukraine "Igor Sikorsky Kyiv Polytechnic Institute" (Kyiv, Ukraine) [14]. The study was conducted at this institution, which is equipped with modern facilities for nanostructural analysis, as well as specialised laboratories, providing a full cycle of studies – from synthesis to spectroscopic and morphological assessment. The samples were synthesised by a hydrothermal method from aqueous solutions under controlled parameters: reaction temperature, reaction duration, reagent concentrations, and the pH of the medium. The starting solutions were prepared from zinc nitrate $Zn(NO_3)_2 \cdot 6H_2O$ (Sigma-Aldrich, USA) and hexamethylenetetramine $C_6H_{12}N_4$ (Merck, Germany) at a concentration of 0.05 mol/L, dissolved in deionised water. The synthesis was carried out at 90 °C for 5 hours in sealed heat-resistant Teflon autoclaves with a volume of 250 ml. After synthesis, the samples were washed with deionised water and dried at 60 °C in a Memmert UF55 drying oven (Germany). The synthesis resulted in the formation of ZnO nanoparticles. The samples for structural and optical characterisation were prepared from the obtained ZnO nanoparticles as powder-derived layers. After drying, the nanopowders were gently dispersed in ethanol and deposited onto clean silicon substrates by drop-casting, followed by drying at room temperature, resulting in discontinuous nanoparticle layers with varying surface coverage. All SEM observations and PL measurements were performed on these layers, while XRD analysis was carried out on the corresponding pow-

der samples to avoid the influence of substrate-related signals. The term “coverage density” in this study refers to the relative surface filling observed in SEM images and is used as a morphological descriptor rather than a parameter of controlled thin-film deposition. Annealing was performed at temperatures of 300, 500, and 700°C for 60 minutes in three different atmospheric conditions – air, nitrogen, and argon. To ensure inert conditions, a Nabertherm RHTH 120/300/16 (Germany) tube furnace was used with gas delivery at a flow rate of 100 ml/min, controlled by a Bronkhorst EL-FLOW (Netherlands) mass flow controller.

The surface morphology was studied by SEM using a JEOL JSM-7001F (Japan) microscope with an accelerating voltage of 15 kV, and the grain size was analysed using ImageJ software (National Institutes of Health, USA) [15] on the basis of images of at least three replicas of each sample. The crystal structure was assessed by XRD on a Rigaku Ultima IV (Japan) diffractometer using CuKα radiation (λ=1.5406 Å); scanning was carried out in the range of 2θ from 20° to 80° at a speed of 2°/min at a voltage of 40 kV and a current of 30 mA.

The luminescent characteristics were studied on an Edinburgh Instruments FLS1000 (United Kingdom) spectrophotometer in the spectral range 300-800 nm; excitation was performed at a wavelength of 325 nm using a laser with a power of 50 mW. The PL spectra were recorded at room temperature; each sample was analysed at least three times to ensure the reliability of the results. Additionally, changes in the intensity and full width at half maximum of the emission peaks as a function of annealing temperature and type of gaseous atmosphere were studied.

For the statistical processing of the experimental data, OriginPro 2021 (OriginLab Corporation, USA) [16] was used. The morphological characteristics (average particle diameter, size dispersion, coverage density) were calculated on the basis of SEM-image analysis by measuring at least 100 nanoparticles for each sample. The average particle size ($\bar{x}$) was calculated according to the standard formula (1):

$$\bar{x} = \frac{1}{n}\sum_{i=1}^{n} x_i \quad \text{.....(1)}$$

where: $\bar{x}$ – the average particle diameter, x_i – the diameter of the i-th particle, n – the number of measured particles.

On the basis of formula (1), the average particle diameters were calculated. Similarly, to assess the variation of particles, the dispersion (σ²) (2) was used:

$$\sigma^2 = \frac{1}{n}\sum_{i=1}^{n}(x_i - \bar{x})^2 \quad \text{.....(2)}$$

where: σ² – the dispersion, $\bar{x}$ – the average particle diameter, x_i – the diameter of the i-th particle, n – the number of measured particles.

In order to assess the reliability of the results, for each parameter the standard deviation (σ) and the 95% confidence interval were also determined, which made it possible to take into account the natural variability of the morphological indicators.

The spectral characteristics (maximum luminescence intensity, full width at half maximum, integral intensity) were evaluated by integrating and approximating the experimental curves using the Gaussian function (3):

$$I(\lambda) = I_o exp\left(\frac{-(\lambda-\lambda_0)^2}{2\sigma^2}\right) \quad \text{.....(3)}$$

where: $I(\lambda)$ – the emission intensity at wavelength λ, I_0 – the maximum intensity (peak amplitude), λ_0 – the position of the maximum, σ – the parameter related to the peak width.

According to the formula (3), the full width at half maximum (FWHM), the position of the maximum (λ_0), and the area under the curve corresponding to the integral emission intensity were determined. These parameters were used in constructing spectral comparisons.

To reveal statistically significant differences between series of samples annealed at different temperatures and in different atmospheric conditions, one-way analysis of variance (ANOVA) was applied, after which Tukey’s test was used for multiple comparison of groups at a significance level of p<0.05. To reveal the correlation between morphological parameters (particle size, degree of aggregation) and luminescent properties (intensity, peak positions), the Pearson correlation coefficient was calculated with the corresponding significance estimate (p<0.05).

Results

As a result of the SEM analysis, the morphological parameters of the nanostructured ZnO samples after heat treatment at temperatures of 300 °C, 500 °C, and 700 °C in three different gaseous atmospheres – air, nitrogen, and argon – were determined. SEM images of ZnO nanoparticles under all annealing conditions are presented in Figure 1.

The Table 1 summarises the average nanoparticle diameter, size dispersion, and substrate coverage density. The data indicate a regular increase in particle size with an increase in annealing temperature, regardless of the atmosphere. The smallest particles (~45 nm) were recorded after annealing in argon at 300 °C, whereas the largest (~112 nm) were recorded at 700 °C in an air atmosphere. At the same time, the coverage density decreased with rising temperature, particularly noticeably under inert conditions (nitrogen, argon), which indicates an increase in nanoparticle aggregation. The particle size dispersion was highest at 700 °C in air, indicating inhomogeneous crystal coalescence in this series of samples (Table 1).

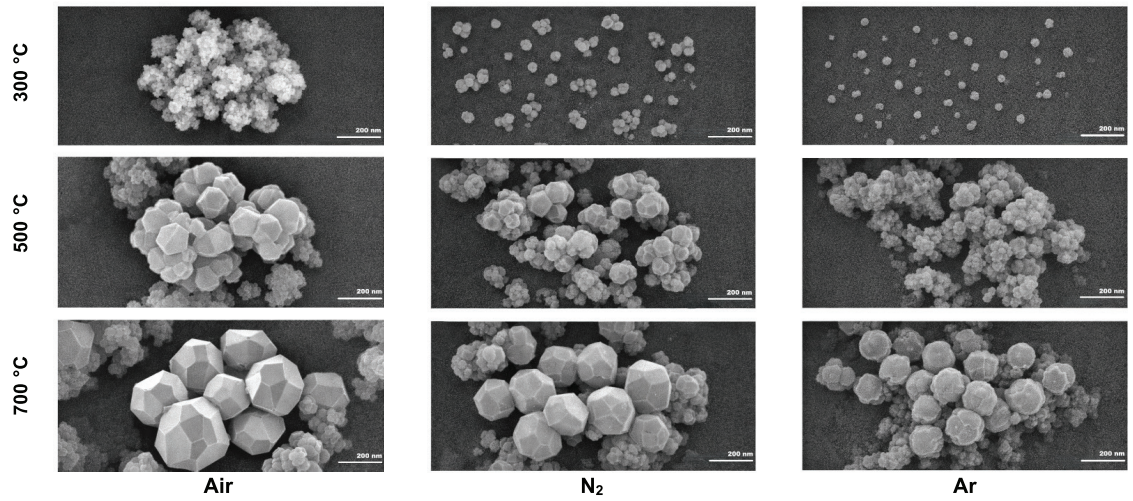

Figure 1. SEM images of ZnO nanoparticles showing morphological evolution under different annealing conditions

Table 1. Morphological parameters of ZnO nanostructures after annealing under different conditions

Temperature (°C)	Atmosphere	Average diameter (nm)	Dispersion (nm²)	Coverage density (%)
300	Air	52±5	45	86
300	Nitrogen	48±4	41	89
300	Argon	45±3	39	91
500	Air	76±6	59	72
500	Nitrogen	71±5	53	75
500	Argon	68±5	50	78
700	Air	112±9	84	54
700	Nitrogen	97±8	72	61
700	Argon	90±7	67	66

Source: compiled by the authors.

The analysis of the morphology of ZnO nanostructures after thermal annealing revealed a significant dependence of nanoparticle parameters on the temperature and gaseous environment of treatment. At a temperature of 300 °C, under all conditions, there was a predominantly isolated granular morphology with particles of spherical or slightly ellipsoidal shape. The smallest average particle sizes (45±3 nm) were obtained in an argon atmosphere, indicating reduced mobility and limited coalescence in an inert environment. Under nitrogen conditions, the average size was 48±4 nm, whereas in air it was slightly larger, 52±5 nm. The size dispersion in this temperature group remained low (up to 45 nm²), indicating a high uniformity of the synthesised structures. The substrate coverage density ranged from 86% to 91%, indicating efficient deposition and the formation of a continuous layer of nanoparticles.

At 500 °C, particle growth processes became noticeably more active, as evidenced by an increase in the average diameter to 76±6 nm (air), 71±5 nm (nitrogen), and 68±5 nm (argon). These changes indicated thermally stimulated surface diffusion and partial grain coalescence. The largest size increase was recorded under conditions of oxygen access, which promotes the intensification of oxidative-diffusion processes, accelerating the aggregation of crystallites. This correlates with a decrease in coverage density to 72% in air, indicating an increase in the gaps between particles due to merging. Under nitrogen and argon, the coverage remained slightly higher (75-78%), but also showed a tendency to decrease.

The most profound morphological changes were found at 700 °C. In this case, the coating structure substantially lost its nanostructured uniformity. In air, the average particle diameter increased to 112±9 nm and the dispersion to 84 nm². This indicates uneven grain growth with the formation of polycrystalline agglomerates of different sizes. The significant variability of shapes and sizes recorded in the SEM images confirms a high degree of thermal coalescence, probably due to the activation of interphase mass-transfer mechanisms under oxidising conditions. In nitrogen and argon environments, the average size was lower – 97±8 nm and 90±7 nm, respectively – indicating a slowdown of aggregation processes. However, even under inert conditions, the coverage density decreased significantly (to 61% and 66%),

demonstrating the inevitability of coalescence at high temperatures regardless of the composition of the gas phase. Thus, the morphological stability of ZnO nanoparticles is ensured only under low-temperature annealing in an inert environment. An increase in temperature promotes particle growth and a reduction in coverage due to thermally induced aggregation, which is intensified in the presence of oxygen [17-20]. The results obtained are of key importance for controlling the morphology of ZnO in optoelectronics, where the preservation of the nanoscale structure is critically important.

X-ray structural analysis of ZnO samples annealed at temperatures of 300 °C, 500 °C, and 700 °C in air, nitrogen, and argon showed the presence of characteristic diffraction maxima corresponding to the hexagonal wurtzite structure (space group $P6_3mc$). The most intense peaks in all samples were the ones with interplanar spacings corresponding to the (100), (002), and (101) planes (Figure 2), with positions of about 31.7°, 34.4°, and 36.2° in 2θ, respectively.

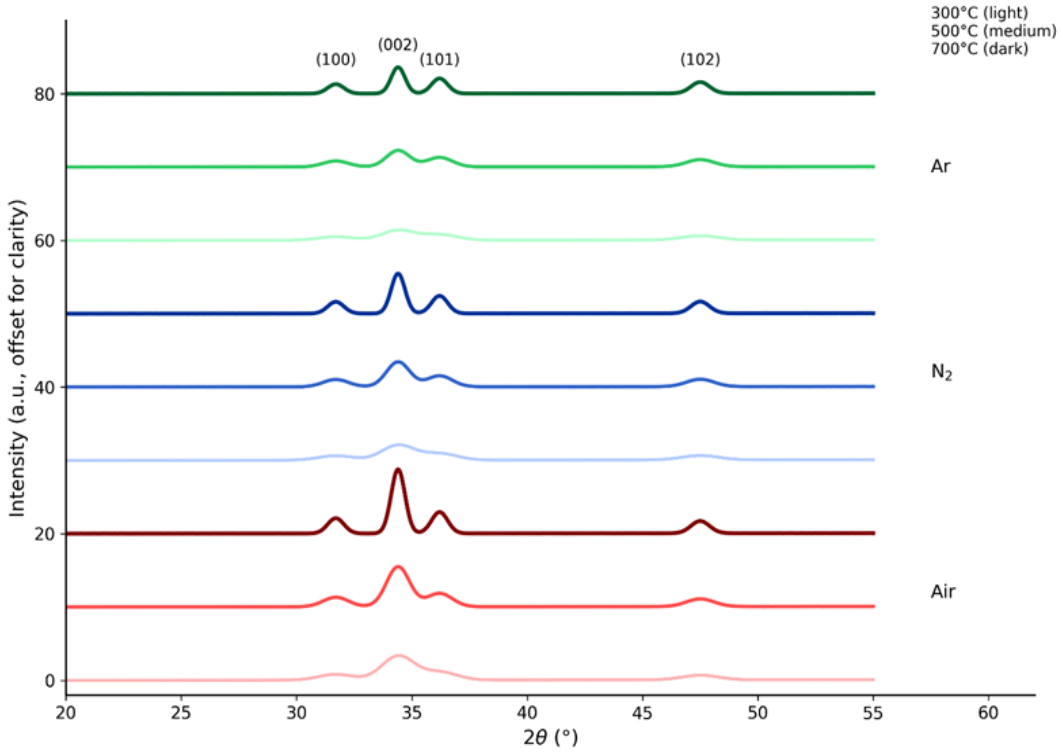

Figure 2. XRD patterns of ZnO nanoparticles annealed at different temperatures in Air, N_2, and Ar atmospheres

Table 2. Parameters of the crystal structure of ZnO determined by the XRD method

Temperature (°C)	Atmosphere	Peak (002), 2θ (°)	Peak width (°)	Crystallite size (nm)
300	Air	34.42	0.29	26
300	Nitrogen	34.41	0.32	24
300	Argon	34.40	0.37	21
500	Air	34.44	0.25	30
500	Nitrogen	34.42	0.27	28
500	Argon	34.41	0.30	26
700	Air	34.45	0.20	38
700	Nitrogen	34.43	0.23	33
700	Argon	34.42	0.25	31

Source: compiled by the authors based on the formula (1).

These values remained unchanged for all heat-treatment conditions, indicating the stability of the ZnO phase composition. However, with increasing temperature, peak narrowing and a decrease in intensity were observed in the samples treated in argon and nitrogen, whereas the samples annealed in air showed the highest intensity and the narrowest peaks. The calculation of the average crystallite size using the Scherrer formula (1) showed an increase in this parameter from ~21 nm (300 °C, argon) to ~38 nm (700 °C, air), which is consistent with the results of the morphological analysis (Table 2).

The obtained X-ray diffractograms of ZnO samples synthesised by the chemical deposition method and annealed at different temperatures and under different atmospheric conditions confirmed the retention of the hexagonal wurtzite structure ($P6_3mc$) in all experimental series. This indicated the high phase stability of ZnO even at elevated temperatures up to 700 °C, regardless of the presence of oxygen in the environment. It should be noted that peak broadening in nanostructured materials is influenced not only by crystallinity but also by crystallite size and microstrain, and therefore cannot be directly interpreted as a decrease in structural order. The main diffraction maxima – particularly the (002) peak located in the range 2θ=34.40°-34.45° – maintained their position within the limits of experimental error, which confirmed the absence of significant changes in the lattice parameters or the formation of new phases.

Despite structural constancy, a detailed analysis of the peak widths and calculations using the Scherrer formula (1) made it possible to identify significant differences in the degree of crystallisation. In the samples annealed at 300 °C, the crystallites were the smallest: 21 nm in argon, 24 nm in nitrogen and 26 nm in air. The broadest peaks (FWHM=0.37°) were observed in the samples annealed in an argon environment, which reflects the combined effect of small crystallite size and lattice microstrain rather than a direct decrease in crystallinity. The inert atmosphere limited the mobility and diffusion of ions, which suppressed coalescence and domain growth, whereas the air atmosphere, with the presence of oxygen, promoted active crystallite growth, a reduction in internal defects, and peak narrowing [21-24]. Raising the temperature to 500 °C led to a noticeable growth of crystallites and a decrease in peak widths in all environments. The effect was particularly clear for the samples treated in air: the peak width decreased to 0.25°, and the average crystallite size reached 30 nm. This is consistent with thermodynamically driven recrystallisation and an increase in the volume of single-crystal fragments. The samples annealed in an inert environment had smaller crystallites (26-28 nm) and broader peaks (up to 0.30°), which indicated the preservation of a significant level of structural defects.

The most pronounced changes were observed at 700 °C. In the samples annealed in air, the diffraction peaks became narrower, and the calculated crystallite size increased, indicating crystallite growth and improved structural ordering. This indicated almost complete coalescence of small crystallites into single grains and a reduction in the concentration of microdefects. The samples treated in argon and nitrogen also showed improvements in crystal quality, although less pronounced (crystallite sizes 31-33 nm; peak widths 0.23-0.25°). This indicated limited grain growth in the absence of oxygen, although the high temperature nevertheless provided sufficient energy for lattice rearrangement. Thus, it was established that high-temperature annealing in an oxidising environment leads to the most pronounced peak narrowing and crystallite growth, indicating improved structural ordering, whereas inert atmospheres slow crystallite growth, preserving the nanoscale. This is of critical importance for applications where a combination of high structural order and controlled nanostructure is required – particularly in optoelectronics and sensor devices.

Spectral PL analysis of ZnO samples annealed at different temperatures in various gaseous environments revealed significant changes in the emission maximum position, intensity, and full width at half maximum (FWHM). All samples exhibited two main luminescence bands: a narrow peak around 380 nm corresponding to near-band-edge emission, and a broader, less intense band in the 510–580 nm region associated with defect-related emission, particularly involving V_O. The intensity of band-edge emission increased significantly with annealing temperature, reaching a maximum at 700 °C in air. In contrast, the samples annealed in inert atmospheres (nitrogen and argon) showed more pronounced defect-related emission, with maxima in the 530–550 nm range. The band-edge peak width was the smallest (FWHM ≈ 22 nm) for the samples annealed at 700 °C in air, indicating high crystalline order and a minimal contribution of defect states, as shown in Figure 3 and summarised in Table 3.

A detailed spectroscopic analysis of the PL characteristics of nanostructured ZnO samples annealed under different atmospheric conditions and at varying temperatures revealed significant correlations between structural order, the defect nature of the samples, and the efficiency of band-edge emission. All series of samples exhibited two-component PL typical of ZnO nanostructures: a narrow maximum in the UV region (~379-395 nm) associated with direct interband recombination, and broadband emission in the visible region (~510-580 nm) caused by point defects – primarily V_O, V_Zn, and interstitial ions.

During annealing at 300 °C, a shift of the band-edge maximum to longer wavelengths was observed – from 387 nm in the samples treated in air to 395 nm in the samples annealed in argon. This red shift indicated a high level of lattice structural defects, leading to the formation of intermediate levels in the band gap, from which recombination occurred with lower energies. The emission intensity in this temperature group remained low, which was related to the high concentration of non-radiative defect states that effectively quenched radia-

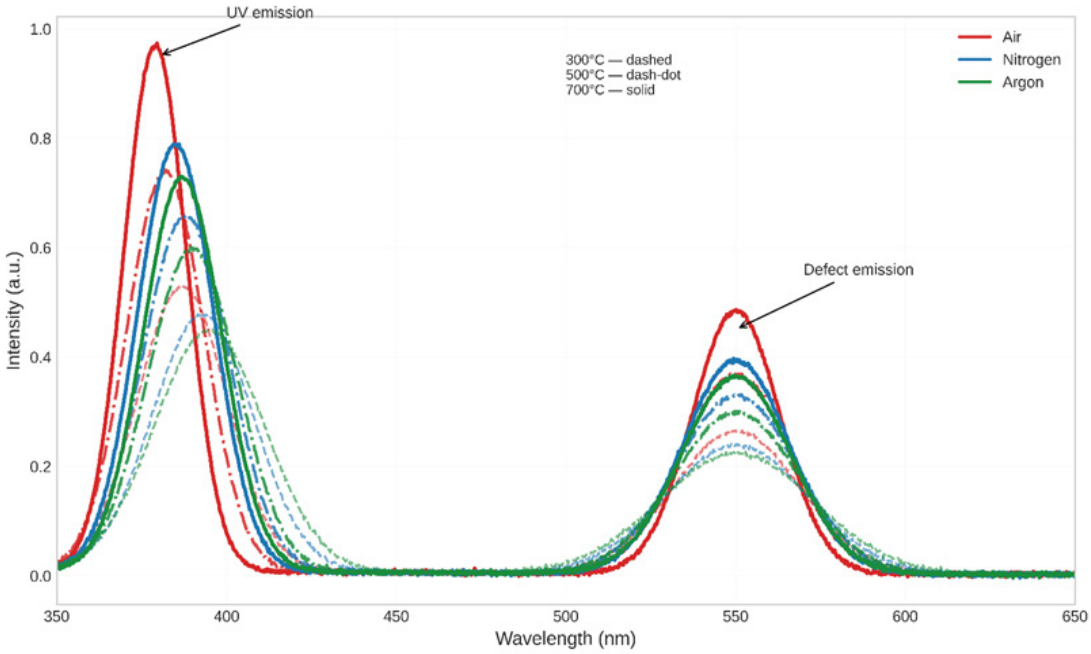

Figure 3. Photoluminescence spectra of ZnO annealed in Air, N_2, and Ar

Table 3. PL parameters of ZnO samples after annealing

Temperature (°C)	Atmosphere	λ_max (nm)	Intensity (relative units)	FWHM (nm)
300	Air	387	0.52	31
300	Nitrogen	393	0.47	35
300	Argon	395	0.44	38
500	Air	382	0.73	27
500	Nitrogen	388	0.65	30
500	Argon	390	0.59	32
700	Air	379	0.96	22
700	Nitrogen	385	0.78	26
700	Argon	387	0.72	28

Source: compiled by the authors based on the formula (3).

tive recombination. The FWHM, which varied from 31 to 38 nm, confirmed the presence of spectral broadening due to structural fluctuations.

Raising the temperature to 500 °C substantially improved the luminescent properties of the samples. In an air environment, the maximum shifted to 382 nm and the intensity increased by almost 40% compared with the lowest values at 300 °C. This indicated active diffusion-driven rearrangement of the crystal lattice, a reduction in the number of deep defects, and the transition of part of the defect centres to a passive state. In the samples annealed in nitrogen and argon, improvements were also observed, though less pronounced – the intensity increased to 0.59-0.65 relative units, and the maximum remained shifted within 388-390 nm. This indicated a limited influence of the inert environment on the efficiency of recrystallisation and defect deactivation.

The most pronounced improvement in PL was recorded at 700 °C. In air, the samples exhibited an emission maximum at 379 nm, corresponding to a near-ideal ZnO band-gap transition, and the intensity reached 0.96 relative units – the highest value among all series. This was accompanied by the narrowest peak (22 nm), which indicated high spectral purity and minimal participation of defect states in the recombination mechanisms. In nitrogen and argon, a shift of the maximum into the violet region (385-387 nm) also occurred, but with less pronounced intensity (0.72-0.78) and peak widths within 26-28 nm. Hence, even in the absence of oxygen, high-temperature annealing led to structural improvement, although it did not ensure the complete elimination of deep defects. The correlation between morphology and luminescence manifested itself through the dependence of intensity and peak width on the average particle size and dispersion. The samples with the smallest size fluctuations (annealed at 700 °C in air) exhibited the narrowest emission, indicating reduced scattering and the homogenisation of energy levels in the material. Thus, the results confirmed that thermal annealing in an oxygen atmosphere is the most effective tool for optimising

the luminescent characteristics of ZnO nanostructures for applications in photonics, sensors, and laser devices.

To identify links between the morphological and optical properties of nanostructured ZnO, Pearson correlation coefficients were calculated between the main morphological parameters (average particle diameter, size dispersion, coverage density) and PL spectral characteristics (maximum band-edge intensity, FWHM, position of λ_max). All calculations were carried out assuming normal distributions and included data for nine experimental conditions (combinations of three temperatures and three annealing atmospheres). A high negative correlation was established between the average particle size and PL intensity (r=-0.89), which indicates that smaller particle sizes are associated with enhanced band-edge emission, likely due to a higher relative contribution of radiative recombination compared to defect-related pathways. Size dispersion showed a positive correlation with peak width (r=0.83), and coverage density had a noticeable positive correlation with PL intensity (r=0.76), indicating the influence of layer homogeneity on emission efficiency. Although these correlations may appear intuitive, the present results provide a quantitative confirmation of the relationship between morphological parameters and luminescent behaviour under controlled annealing conditions, while also allowing their combined influence to be considered rather than treated as isolated effects (Table 4).

Table 4. Pearson correlation coefficients between morphological and spectral parameters of ZnO

Parameter 1	Parameter 2	r	Significance (p)
Average particle diameter	PL intensity	-0.89	<0.01
Size dispersion	FWHM	0.83	<0.05
Coverage density	PL intensity	0.76	<0.05
Average particle diameter	Maximum position (λ_max)	0.68	<0.05
Size dispersion	PL intensity	-0.65	<0.05
Coverage density	FWHM	-0.61	<0.05

Source: compiled by the authors.

Correlation analysis between the morphological parameters (average particle size, dispersion, coverage density) and the luminescent characteristics (intensity, position of the emission maximum, peak width) of ZnO nanostructures provided a deeper understanding of the mechanisms that determine the efficiency and quality of emission depending on the structural properties of the material. One of the strongest links identified was the negative correlation between average particle size and PL intensity (r=-0.89, p<0.01). This indicated that with a decrease in crystallite size, the quantum efficiency of band-edge emission increased markedly. Such an effect may be due to a combination of several factors: an increase in specific surface area, improved spatial confinement of electrons and holes, a reduction in the probability of exciting defect levels, and a limitation of the volume in which defects can accumulate.

Another important observation was the positive correlation between substrate coverage density and PL intensity (r=0.76, p<0.05). A high coverage density indicates a homogeneous distribution of nanoparticles over the surface, which reduces emission scattering and provides efficient pathways for excitation transfer within the structure. Such conditions are particularly important for sensing and emitting applications, where the uniformity and coherence of the material directly affect the stability and intensity of the signal. Size dispersion also showed a strong positive correlation with the spectral peak width (r=0.83, p<0.05). This indicated that increased morphological inhomogeneity causes a broadening of the energy levels involved in recombination, leading to reduced monochromaticity and selectivity of the emission. Such an effect adversely affects devices that require narrowband or coherent emission, in particular, laser or photodetector components.

Additionally, the correlation found between the average diameter of nanoparticles and the position of the emission maximum (r=0.68, p<0.05) cannot be attributed to quantum confinement, since the particle sizes in this study (30-100 nm) are significantly larger than the exciton Bohr radius of ZnO (~2-3 nm). Instead, the shift of the emission maximum is more likely associated with variations in defect structure and surface states, which influence the recombination pathways. This makes it possible to tune the spectral position of the emission by changing the crystallite sizes, which is relevant for creating light sources with a tailored wavelength. On the other hand, the negative correlation between dispersion and intensity (r=-0.65, p<0.05), as well as between coverage density and spectral width (r=-0.61, p<0.05), indicates the need for structural homogeneity to achieve an optimal PL response. High dispersion and low coverage can create inhomogeneous regions that act as sources of non-radiative losses, degrading emission quality [25-28].

In summary, the statistically significant links identified have critical applied significance. The links indicate the possibility of controlling the luminescent properties of ZnO through morphology engineering – the control of synthesis and thermal-treatment conditions makes it possible to increase the intensity, narrowband character, and spectral position of the emission without additional doping. This opens up prospects for the creation of highly efficient optoelectronic devices, sensors, UV light sources, and biosensing systems based on structured ZnO.

Discussion

The conducted study confirmed that the morphological and structural properties of ZnO nanoparticles were closely dependent on the annealing temperature and the composition of the gas atmosphere. With increasing temperature, a systematic increase in the average particle size and a decrease in the surface coverage were observed, particularly pronounced in inert environments, indicating the activation of aggregation processes. A similar dependence was described by Lekoui et al. [29] and Dlamini et al. [30], who noted a decrease in the density of the nanostructured ZnO layer at temperatures above 600 °C owing to particle coalescence. However, the present study additionally demonstrated an increase in size dispersion at high temperatures, especially in air, which was not considered in the works of Lekoui et al. [29] and Dlamini et al. [30], and therefore provided a more comprehensive understanding of the thermal mechanisms governing morphology formation.

The crystalline structure of ZnO remained stable regardless of the annealing conditions, retaining the hexagonal wurtzite phase [31-33]. This was consistent with the conclusions of Mohapatra and Kushwaha [34], who indicated the high phase stability of ZnO under thermal treatment. However, unlike the results of Ho et al. [35], who did not record significant changes in peak widths with increasing temperature, the present study revealed pronounced peak narrowing, especially in an air environment. This indicated a significant improvement in crystallinity, confirming active crystallite growth and a reduction in internal structural defects under the influence of oxygen.

The atmospheric conditions substantially affected the degree of recrystallisation: according to X-ray diffraction data, in an inert environment, the crystallites remained smaller and exhibited broader diffraction peaks. This effect correlated with the conclusions of Zhang et al. [36] and Juan et al. [37], who pointed to limited ion diffusion in the absence of oxygen. At the same time, in contrast to the conclusions about the minor influence of the gas phase, the present study showed a substantial difference in crystallite size and peak width, indicating greater sensitivity of ZnO to the synthesis atmosphere than previously assumed.

The PL properties of ZnO, according to the results presented, showed a clear dependence on morphology and the degree of structural defects. The highest intensity and the narrowest peaks of band-edge emission were achieved at 700 °C in an oxygen atmosphere, indicating a high degree of structural order. These data confirmed the observations of Nkosi et al. [38], who found a similar trend in ZnO thin films, and Majumder et al. [39], who established the role of oxygen in defect deactivation. At the same time, the results in inert environments differed substantially: defect-related luminescence dominated, indicating the persistence of structural defectiveness even at high temperatures.

In contrast to Wong et al. [40], who reported a minor influence of the environment on spectral characteristics at 500 °C, the present study showed distinct shifts of maxima and changes in intensity, demonstrating the critical role of an oxidising atmosphere in reduction of defect states. Thus, the results provided deeper insight into the spectroscopic understanding of ZnO and showed greater variability of the PL response depending on the conditions of heat treatment.

Correlation analysis confirmed the presence of a close link between morphology and luminescence, in particular, a negative correlation between the average particle diameter and PL intensity. Similar dependencies were described by Van Thai et al. [41] and Sun et al. [42], who explained the increase in intensity with decreasing particle size by quantum-confinement effects. However, in the present study, such effects are unlikely, since the particle sizes exceed the range where quantum confinement is significant. Instead, the observed trends are attributed to changes in defect structure and recombination dynamics, which influence the optical response of ZnO.

The positive correlation between surface coverage and emission intensity confirmed the results of Camacho-Espinoza et al. [43], who showed the influence of nanolayer homogeneity on the efficiency of excitation transfer. A high density of particles on the surface ensured a reduction of inhomogeneities in excitation transfer, lowering energy losses associated with scattering, and promoted the formation of a coherent photon flux. In addition, such a configuration provided better interaction between nanoparticles and the electromagnetic field, which increased the probability of radiative recombination. At the same time, Szyszka and Wiglusz [44] did not find a significant relationship between particle distribution and PL properties, arguing that intracrystalline defects dominated over morphological factors. However, the data of the present study demonstrated that it was precisely the regularity and density of the nanostructured layer that had a key influence on emission efficiency, indicating the importance of structural coherence as a critical factor. Thus, the results of the study complemented the existing scholarly discussion, pointing to the need to consider morphological homogeneity not only as an aesthetic or statistical parameter, but as a physically relevant characteristic that determines the optical performance of ZnO-based materials.

The presence of a positive correlation between dispersion and spectral peak width indicated a broadening of energy levels in the case of morphological inhomogeneity. A similar observation was made in the studies of Hedl et al. [45] and Ati et al. [46], who investigated the dependence of emission selectivity on fluctuations in nanoparticle sizes. However, unlike those works, the present study also revealed a negative relationship between coverage density and peak width, indicating an additional influence of spatial structure on spectral purity.

The analysis results showed that effective PL was achieved under conditions of minimal dispersion, high

surface coverage, and small average particle diameter. This enabled targeted modification of synthesis parameters in order to obtain materials with the desired optical properties. Such a conclusion was consistent with the propositions of Wei et al. [47], who proposed the concept of morphological engineering to control photonic properties, and Zhang et al. [48], who experimentally confirmed the significance of morphological factors in the generation of intense UV emission.

It should be noted separately that under high-temperature conditions, even an inert environment led to partial crystallite coalescence, which limited the preservation of the nanoscale structure. This observation contradicted the conclusions of Gherab et al. [49], who claimed the possibility of stabilising the nanoscale properties of ZnO at 700 °C in argon. The data presented indicated that, although particle growth in an inert environment was less intense, it nevertheless significantly reduced surface coverage and structural homogeneity.

The obtained results have significant practical relevance for the creation of optoelectronic devices where high crystallinity and the preservation of a nanostructured state were simultaneously required. It was confirmed that the atmospheric environment of heat treatment was a critical parameter determining the balance between crystallite growth and the level of structural defects, which affected both structural stability and optical efficiency. When using an oxidising environment at high temperatures, an improvement in crystallinity and a reduction in defects were observed, which promoted enhanced band-edge emission, whereas inert atmospheres allowed the nanoscale to be preserved but were accompanied by lower lattice order. Such an approach was also supported by Negi et al. [50] and Li et al. [51], who regarded the gas phase as a key factor in regulating the photonic properties of metal oxides, emphasising its significance for ensuring the stability of electronic states and reducing the level of surface defects. The study also showed that reducing particle size did not always ensure high emission quality if accompanied by an increase in dispersion or a decrease in surface coverage. These factors could lead to an inhomogeneous distribution of energy levels and an increase in non-resonant losses, which was not considered in the model of Karahan et al. [52] and Sprincean et al. [53], which focused exclusively on the size factor without taking morphological homogeneity into account.

Thus, a comparative analysis of the morphological, structural, and PL characteristics of ZnO nanostructures under different heat-treatment conditions made it possible to draw conclusions about the optimal parameters for the practical application. Lowering the annealing temperature in combination with an inert atmosphere ensured the preservation of the nanostructured state, but only at the expense of crystallinity. At the same time, a high temperature in combination with an oxygen atmosphere provided the best optical characteristics but promoted aggregation. In this context, it is advisable to search for compromise synthesis regimes or additional methods of structural stabilization.

Conclusions

The conducted study demonstrated the influence of annealing temperature and gas-atmosphere composition on the morphological, structural, and optical characteristics of nanostructured ZnO. SEM analysis showed that with an increase in treatment temperature from 300 °C to 700 °C, there was a significant increase in the average diameter of nanoparticles (from ~45 nm to ~112 nm) and a decrease in surface coverage from 91% to 54%, indicating the occurrence of coalescence and aggregation processes. The smallest particle sizes and the highest coverage density were obtained under an inert argon atmosphere at 300 °C, which indicated the preservation of nanostructural integrity at low temperature and in the absence of oxygen.

XRD analysis confirmed the preservation of the hexagonal wurtzite phase regardless of conditions; however, the intensity and width of the diffraction peaks varied depending on temperature and atmosphere. The maximum crystallite size (~38 nm) and the minimum diffraction-peak width (~0.20°) were recorded after thermal treatment in air at 700 °C, indicating an increased degree of recrystallisation and a reduction in the concentration of structural defects. Spectral PL analysis showed that the intensity of band-edge emission increased significantly with increasing temperature, reaching a maximum at 700 °C in air (0.96 rel. units) with a minimum peak width (22 nm). In inert environments, defect-related luminescence dominated, accompanied by lower intensity and broader spectral bands.

The optimal conditions for obtaining high-quality ZnO nanostructures with pronounced optical properties were identified as annealing at 700 °C in an oxygen atmosphere. Such structures were recommended for use in UV LEDs, photodetectors, and sensors, where the combination of nanoscale morphology and high crystallinity was critical. The limitations of the study lay in focusing only on the influence of temperature and gas atmosphere without taking into account other synthesis factors such as annealing time, type of precursors, and substrate geometry. The possible influence of doping on spectral properties was also not considered. In further studies, it would be appropriate to expand the parametric space and investigate the long-term stability of the structures during operation.

References

[1] Vasin A, Kysil D, Rusavsky A, Isaieva O, Zaderko A, Nazarov A, Lysenko V. Synthesis and luminescent properties of carbon nanodots dispersed in nanostructured silicas. *Nanomaterials.* 2021, 11(12), 3267. https://doi.org/10.3390/nano11123267

[2] Ratov BT, Mechnik VA, Bondarenko NA, Kolodnitskyi VM,

Gevorkyan ES, Nerubaskyi VP, Gusmanova AG, Fedorov BV, Kaldibaev NA, Arshidinova MT, Kulych VG. Features Structure of the Cdiamond–(WC–Co)–ZrO2 Composite Fracture Surface as a Result of Impact Loading. *Journal of Superhard Materials*. 2023, 45(5), 348–359. https://doi.org/10.3103/S1063457623050088

[3] Mostovshchikov AV, Ilyin AP, Zabrodina IK, Root LO, Ismailov DV. Measuring the changes in copper nanopowder conductivity during heating as a method for diagnosing its thermal stability. *Key Engineering Materials.* 2018, 769, 146–151. https://doi.org/10.4028/www.scientific.net/KEM.769.146

[4] Ibrahimova HS, Rzayev RM, Mustafayeva EM. Thermophyical Properties PP/ZrO2 Nanocomposites Before and After Electrothermal Polarization. *Journal of Inorganic and Organometallic Polymers and Materials*. 2024. https://doi.org/10.1007/s10904-024-03062-y

[5] Fialko NM, Navrodska RO, Shevchuk SI, Gnedash GO. The environmental reliability of gas-fired boiler units by app lying modern heat-recovery technologies. *Naukovyi Visnyk Natsionalnoho Hirnychoho Universytetu*. 2020, 2020(2), 96–100. https://doi.org/10.33271/nvngu/2020-2/096

[6] Michailovska K, Indutnyi I, Shepeliavyi P, Sopinskyy M, Danko V, Tsybrii Z, Maziar D. Formation of silicon nanocomposites by annealing of (SiOx/Sm)n multilayers: Luminescence, Raman and FTIR studies. *Applied Nanoscience.* 2023, 13(20), 7187–7194. https://doi.org/10.1007/s13204-023-02887-2

[7] Hristov H, Baneva Y, Nedeva D, Arhangelova N, Penev I, Velev V, Moschini G, Rossi P, Uzunov NM. Thermoluminescence properties of Eu and Li co-doped Gd2O 3, induced by UV light. *Journal of Physics Conference Series.* 2012, 398(1), 012043. https://doi.org/10.1088/1742-6596/398/1/012043

[8] Kryshtab T, Borkovska L, Cortés Herrera R, Kryvko A, Kolomys O, Mamykin S, Portier X. Influence of terbium doping and annealing on the structural and optical characteristics of sputtered zinc oxide thin films. *Crystals.* 2023, 13(8), 1200. https://doi.org/10.3390/cryst13081200

[9] Talla A, Suliali N, Goosen W, Urgessa Z, Motloung S, Botha J. Effect of annealing temperature and atmosphere on the structural, morphological and luminescent properties of TiO2 nanotubes. *Physica B: Condensed Matter.* 2022, 640, 414026. https://doi.org/10.1016/j.physb.2022.414026

[10] Buryi M, Remeš Z, Babin V, Artemenko A, Vanecek V, Dragounová K, Landová L, Kučerková R, Mičová J. Transformation of free-standing ZnO nanorods upon Er doping. *Applied Surface Science.* 2021, 562, 150217. https://doi.org/10.1016/J.APSUSC.2021.150217

[11] Desouky F, Abou-Helal M. Synthesized nanostructures of oxostannate Cs2Sn2O3 with a prospective study of structural, electrical, optical, and luminescence properties: Effect of annealing temperature. *Journal of Inorganic and Organometallic Polymers and Materials.* 2024, 34(12), 6211–6226. https://doi.org/10.1007/s10904-024-03185-2

[12] Sharma L, Sahare P. Mechanoluminescence, thermoluminescence, optically stimulated luminescence and photoluminescence in SrAl2O4:Eu micro- and nanophosphors: Effect of particle size and annealing in different atmospheres. *RSC Advances.* 2023, 13(36), 25579–25598. https://doi.org/10.1039/d3ra02514d

[13] Roselló-Márquez G, Fernández-Domene R, Sánchez-Tovar R, García-Antón J. Influence of annealing conditions on the photoelectrocatalytic performance of WO3 nanostructures. *Separation and Purification Technology*. 2020, 238(9), 116417. https://doi.org/10.1016/j.seppur.2019.116417

[14] National Technical University of Ukraine “Igor Sikorsky Kyiv Polytechnic Institute”. 2025. https://kpi.ua/en/

[15] National Institutes of Health. 2025. ImageJ. https://imagej.net/ij/docs/intro.html

[16] OriginLab Corporation. 2025. OriginPro 2021. https://www.originlab.com/2021

[17] Borisov YuS, Korzhik VN, Gritskiv YaP, Kunitskii YuA. Structural transformations occurring in flame-sprayed Ni60Nb40 alloy coatings during heating in the presence of oxygen. *Soviet Powder Metallurgy and Metal Ceramics.* 1987, 26(12), 966–970. https://link.springer.com/article/10.1007/BF00797782

[18] Kunitskii YuA, Korzhik VN, Nemirovskii AV. Transformations in the plasma-sprayed Fe67Ti7B24C2 alloy in heating. *Soviet Materials Science.* 1990, 26(1), 87–90. https://link.springer.com/article/10.1007/BF00734547

[19] Nikolov N, Pashkouleva D, Yanakieva A. Identification of mechanical characteristics of an amorphous metallic material. *Comptes Rendus de L'Academie Bulgare des Sciences.* 2013, 66(1), 119–126. https://doi.org/10.7546/CR-2013-66-1-13101331-15

[20] Kadyrzhan K, Suleimenov I, Tolymbekova L, Seitenova G, Kopishev E. Background of New Measurement Electronic Devices with Polyelectrolyte Hydrogel Base. *Polymers.* 2025, 17(4), 539. https://doi.org/10.3390/polym17040539

[21] Yakovkin IN, Katrich GA, Loburets AT, Vedula YuS, Naumovets AG. Alkaline-earth overlayers on furrowed transition metal surfaces: An example of tailoring the surface properties. *Progress in Surface Science*. 1998, 59(1-4), 355-365. https://doi.org/10.1016/S0079-6816(98)00061-6

[22] Loburets AT, Naumovets AG, Vedula YuS. Diffusion of dysprosium on the (112) surface of molybdenum. *Surface Science.* 1998, 399(2-3), 297-304. https://doi.org/10.1016/S0039-6028(97)00830-3

[23] Sevdimaliyev YM, Salmanova GM, Akbarli RS, Nagieva NB. Propagation of waves in a hydroelastic shell-viscous liquid system, in the presence of gas bubbles. *Mathematical Methods in the Applied Sciences.* 2023, 46(12), 12176–12189. https://doi.org/10.1002/mma.8202

[24] Akbarov SD, Akbarli RS. Dispersion of Quasi-Scholte Waves in a Hydroelastic System Consisting of an Orthotropic Plate and a Compressible Fluid Layer. *Mechanics of Composite Materials.* 2025, 60(6), 1225–1238. https://doi.org/10.1007/s11029-025-10256-z

[25] Horbachova O, Buiskykh N, Mazurchuk S, Lomaha V. Acetylation of Aspen and Alder Wood. Preliminary Tests. *Key Engineering Materials.* 2024, 986, 45–52. https://doi.org/10.4028/p-d9fYLX

[26] Shattnan AT, Musa KM, Alkaabi AA. The use of unsaturated nano-polyester to prepare chlorine halogenated polymers. *Journal of Computational and Theoretical Nanoscience.* 2019, 16(1), 124–129. https://doi.org/10.1166/jctn.2019.7710

[27] Uzunov N, Hristov H, Velev V, Arhangelova N, Bozadzhiev V, Nedeva D, Penev I. Assessment of Trap Parameters Related with Thermoluminescence Peaks in BGO Single Crystals Doped with Vanadium. International *Journal of Recent Technology and Engineering* (IJRTE). 2015, 4(1), 12–15. https://www.researchgate.

net/publication/377276489_Assessment_of_Trap_Parameters_Related_with_Thermoluminescence_Peaks_in_BGO_Single_Crystals_Doped_with_Vanadium
[28] Horbachova O, Mazurchuk S, Buiskykh N, Lomaha V, Matviichuk A. Effect of the operating environment conditions of wood composites on the adhesive joint strength. *Ukrainian Journal of Forest and Wood Science.* 2024, 15(4), 56–71. https://doi.org/10.31548/forest/4.2024.56
[29] Lekoui F, Amrani R, Filali W, Garoudja E, Sebih L, Bakouk I, Akkari H, Hassani S, Saoula N, Oussalah S, Albalawi H, Alwadai N, Henini M. Investigation of the effects of thermal annealing on the structural, morphological and optical properties of nanostructured Mn doped ZnO thin films. *Optical Materials.* 2021, 118, 111236. https://doi.org/10.1016/J.OPTMAT.2021.111236
[30] Dlamini C, Mhlongo M, Koao L, Motaung T, Hlatshwayo T, Motloung S. The effects of varying the annealing period on the structure, morphology and optical properties of MgAl2O4:0.1% Mn2+ nanophosphors. *Applied Physics* A. 2020, 126(1), 75. https://doi.org/10.1007/s00339-019-3248-7
[31] Borisov YuS, Kunitskii YuA, Korzhik VN, Yaprakova MG. Structure and some physical properties of plasma-sprayed coatings of the nickel boride Ni3B. *Soviet Powder Metallurgy and Metal Ceramics.* 1986, 25(12), 966–969. https://link.springer.com/article/10.1007/BF00797102
[32] Abbasova GG, Ismayilov RH, Tagiyev DB, Şenol H, Song Y, Medjidov AA, Huseynova MT, Fatullaeva PA, Taslimi P, Sadeghian N, Lee G-H, Peng S-M. Synthesis, characterization, crystal structure, molecular dynamics simulations, MM-GBSA analysis, and bioactivity studies of pyrazine- and pyrimidine-modulated unsymmetrical dipyridylamide complexes. *Journal of Molecular Structure.* 2024, 1315, 138896. https://doi.org/10.1016/j.molstruc.2024.138896
[33] Guseinova KM, Mammadov FA, Hadiyeva AA, Eminova VI, Huseynov CI. Energy of crystal lattice thermal oscillations in tlgas2 semiconductor compound. *East European Journal of Physics.* 2024, 2024(4), 322–328. https://doi.org/10.26565/2312-4334-2024-4-36
[34] Mohapatra L, Kushwaha A. Annealing atmospheres induced structural and morphological transformation of zinc tin hydroxide nanostructures. *Ceramics International*. 2023, 49(10), 15154–15163. https://doi.org/10.1016/j.ceramint.2023.01.098
[35] Ho C, Yu C, Yang C. Effects of annealing temperature on morphology and LSPR sensing performance of Au nanostructures. In: *2024 IEEE SENSORS* (pp. 1–3). Kobe: Institute of Electrical and Electronics Engineers, 2024. https://doi.org/10.1109/SENSORS60989.2024.10784824
[36] Zhang R, Kajita S, Hwangbo D, Sinelnikov D, Tanaka H, Ohno N. Changes in morphology and field emission property of nano-tendril bundles after high temperature annealing. *Nuclear Materials and Energy.* 2022, 31, 101178. https://doi.org/10.1016/j.nme.2022.101178
[37] Juan J, Bravo A, Federico J, Rios R, Sánchez A, Moreno M, Huerta L. Effect of the thermal annealing temperature on the luminescent and morphological properties of silicon rich oxide bilayer structures. In: *2023 IEEE Latin American Electron Devices Conference* (pp. 1–4). Puebla, Institute of Electrical and Electronics Engineers, 2023. https://doi.org/10.1109/LAEDC58183.2023.10209139
[38] Nkosi S, Kortidis I, Motaung D, Kroon R, Leshabane N, Tshilongo J, Ndwandwe O. The effect of stabilized ZnO nanostructures green luminescence towards LPG sensing capabilities. *Materials Chemistry and Physics.* 2020, 242, 122452. https://doi.org/10.1016/j.matchemphys.2019.122452
[39] Majumder S, Gu M, Kim K. Effect of annealing of β-Bi2O3 over enhanced photoelectrochemical performance. *Materials Science in Semiconductor Processing.* 2022, 141, 106439. https://doi.org/10.1016/j.mssp.2021.106439
[40] Wong C, Whaley J, Wada T, Harayama S, Oya Y, Kolasinski R. Changes in surface morphology of helium-induced tungsten nanostructure during high-temperature annealing. *Nuclear Materials and Energy.* 2020, 22, 100730. https://doi.org/10.1016/j.nme.2020.100730
[41] Van Thai C, Dung N, Van Hai N, Minh V, Xuan T, Tuan P, Van Huan P, Van H. Intense green upconversion emission of rare-earth-doped Sr3(PO4)2/Sr2P2O7 powder: Effect of annealing temperature and temperature-sensor properties. *Optik.* 2022, 264, 169446. https://doi.org/10.1016/j.ijleo.2022.169446
[42] Sun Y, Jian Y, Yang S, Chiang P, Su C. Structural evolution and nanodomain formation in blend films of a block copolymer and homopolymer. *Soft Matter.* 2024, 21(2), 277–290. https://doi.org/10.1039/d4sm01029a
[43] Camacho-Espinoza M, Fernández-Osorio A, Tapia M, Casanova R, Huerta L. Effect of annealing temperature on the properties and the chromium oxidation state of ZnAl1.94Cr0.06O4 nanoparticles prepared by coprecipitation method. *Journal of Solid State Chemistry.* 2024, 336, 124741. https://doi.org/10.1016/j.jssc.2024.124741
[44] Szyszka K, Wiglusz R. Impact of dopant concentration on the structural, morphological, and spectroscopic characteristics of Eu3+-Doped Sr10(PO4)6F2 nanomaterials, including temperature-dependent emission. *Journal of Alloys and Compounds*. 2024, 984, 173924. https://doi.org/10.1016/j.jallcom.2024.173924
[45] Hedl E, Bregović V, Rakić I, Mandić Š, Samec Ž, Bergmann A, Sancho-Parramon J. Optical properties of annealed nearly percolated Au thin films. *Optical Materials*. 2023, 135, 113237. https://doi.org/10.1016/j.optmat.2022.113237
[46] Ati A, Abdalsalam A, Abbas H. Influence of annealing on structural, morphology, magnetic and optical properties of PLD deposited CuFe2O4 thin films. *Inorganic Chemistry Communications. 2022, 146, 110072. https://doi.org/10.1016/j.ino*che.2022.110072
[47] Wei D, Bai J, Huang Y, Seo H. Surface oxygen defects induced via low-temperature annealing and its promotion to luminescence and photocatalysis of Eu3+-doped Te3Nb2O11 nanoparticles. *Applied Surface Science.* 2020, 533, 147502. https://doi.org/10.1016/j.apsusc.2020.147502
[48] Zhang J, Lu J, Hou P, Liu Y, Li Z, Lu P, Wen G, Liu L, Sun H. Structural, optical and singular magnetic properties of anodized titanium dioxide nanotubes. *Journal of Alloys and Compounds.* 2023, 952, 170010. https://doi.org/10.1016/j.jallcom.2023.170010
[49] Gherab K, Al-Douri Y, Hashim U, Khenata R, Bouhemadou A, Ameri M. Temperature effect to investigate optical and structural properties of AZO nanostructures for optoelectronics. *Bulletin of Materials Science*. 2021, 44(1), 39. https://doi.org/10.1007/s12034-020-02298-x
[50] Negi D, Shyam R, Shekhawat K, Vashishtha P, Gupta

G, Gupta M, Nelamarri S. Investigation of structural modification, surface chemical states, and luminescence behavior of rapid thermal annealing treated MgTiO3 thin films. *Journal of Materials Science: Materials in Electronics.* 2023, 34(14), 1165. https://doi.org/10.1007/s10854-023-10553-0

[51] Li M, Liu Y, Zhang Y, Han X, Zhang T, Zuo Y, Xie C, Xiao K, Arbiol J, Llorca J, Ibáñez M, Liu J, Cabot A. Effect of the annealing atmosphere on crystal phase and thermoelectric properties of copper sulfide. *ACS Nano.* 2021, 15(3), 4967–4978. https://doi.org/10.1021/acsnano.0c09866

[52] Karahan O, Tufani A, Unal S, Misirlioglu I, Menceloğlu Y, Şendur K. Synthesis and morphological control of VO2 nanostructures via a one-step hydrothermal method. *Nanomaterials.* 2021, 11(3), 752. https://doi.org/10.3390/nano11030752

[53] Sprincean V, Qiu H, Lupan O, Tjardts T, Petersen D, Veziroglu S, Adelung R, Caraman M. Synthesis and properties of β-Ga2O3 nanowires and nanosheets on doped GaS:Mn substrates. *Materials Science in Semiconductor Processing.* 2024, 172, 108040. https://doi.org/10.1016/j.mssp.2023.108040

Izvod

UTICAJ TEMPERATURE I ATMOSFERE ŽARENJA NA MORFOLOGIJU I LUMINESCENTNA

Viktor Zavodyannyi[1], Mykola Voloshyn[1], Valentina Zubenko[1], Roman Kovalenko[1], Serhii Rahulin[1]

[1]Katedra za hidrotehniku, vodotehniku i elektrotehniku, Hersonski državni agrarno-ekonomski univerzitet, Kropivnicki, Ukrajina

(ORIGINALNI NAUČNI RAD)
UDK: 66,017/018
DOI: 10.5937/savteh2601057Z

Cilj ovog rada bio je da se utvrdi na koji način temperatura i gasna atmosfera tokom žarenja utiču na morfološka i luminescentna svojstva nanostrukturnih materijala na bazi cink-oksida (ZnO). Istraživanje je sprovedeno u Ukrajini, na Nacionalnom tehničkom univerzitetu Ukrajine Igor Sikorsky Kyiv Polytechnic Institute“. Metodologija je obuhvatila hemijsku depoziciju iz vodenih rastvora, nakon čega je usledilo termičko žarenje na 300, 500 i 700 °C u atmosferi vazduha, azota i argona. Morfologija je analizirana skenirajućom elektronskom mikroskopijom (SEM), kristalna struktura difrakcijom rendgenskih zraka (XRD), dok su luminescentni spektri ispitivani spektroskopijom fotoluminescencije (PL). Rezultati su pokazali povećanje veličine čestica sa porastom temperature, nezavisno od atmosfere žarenja, pri čemu je najmanja veličina čestica (~45 nm) zabeležena na 300 °C u argonu, a najveća (~112 nm) na 700 °C u vazduhu. Sa povećanjem temperature smanjivala se gustina pokrivenosti, naročito u inertnim uslovima, usled agregacije nanočestica. Korelaciona analiza pokazala je snažnu negativnu povezanost između veličine čestica i intenziteta emisije (r = –0,89), kao i pozitivnu korelaciju između gustine pokrivenosti i intenziteta PL emisije (r = 0,76). Na osnovu toga je utvrđeno da visokotemperaturno žarenje u atmosferi kiseonika najefikasnije poboljšava luminescentne karakteristike ZnO, što je značajno za optoelektronske i senzorske primene. Dobijeni rezultati imaju praktičan značaj za razvoj visokoefikasnih optoelektronskih i senzorskih uređaja.

Ključne reči: gustina sloja, spektralna čistoća, veličina kristalita, intenzitet emisije, defekti rešetke, cink-oksid.

CRediT authorship contribution statement:
Viktor Zavodyannyi: Conceptualization, study design, supervision, data curation, writing – original draft preparation.
Mykola Voloshyn: Methodology development, validation, formal analysis, writing – review and editing.
Valentina Zubenko: Investigation, data analysis, visualization, writing – review and editing.
Roman Kovalenko: Data collection, statistical analysis, preparation of figures and tables, writing – review and editing.
Serhii Rahulin: Experimental work, software and instrumentation support, writing – review and editing.